26th Symposium on Naval Hydrodynamics
Rome, Italy, 17-22 September 2006

Nonlinear surface wave dynamics in slowly varying ocean environments

Wooyoung Choi[1] and David R. Lyzenga[2]
([1]New Jersey Institute of Technology, [2]University of Michigan, USA)

ABSTRACT

A theoretical model is developed to study the evolution of nonlinear surface waves interacting with slowly-varying surface currents and bottom topography. The model is then solved numerically using a pseudo-spectral method. Our numerical solutions for the evolution of both periodic standing waves and solitary waves for the case of uniform water depth are validated with fully nonlinear numerical solutions of the Euler equations. For a uniform surface wave train interacting with a slowly varying surface current, the local wave number and wave amplitude are computed from our numerical solutions of the model and show good agreement with those of the wave action model. It is shown that the nonlinear model can be further generalized to include the effect of slowly-varying bottom topography of arbitrary amplitude.

1 INTRODUCTION

Computing the evolution of highly time-dependent, three-dimensional, nonlinear surface wave fields accurately in nonuniform ocean environments is one of the most challenging hydrodynamic problems. The energy transfer between different length scales is a complex physical process, and the understanding of nonlinear wave-wave interaction is still far from complete when surface waves are interacting with nonuniform currents and bottom topography. In this paper, a formulation is presented to incorporate wave-current interaction and bottom topography effects into the nonlinear wave prediction model, and the evolution of nonlinear surface gravity waves is studied numerically.

In the absence of surface currents and bottom topography, the free surface elevation, $\zeta(\boldsymbol{x},t)$, and the free surface velocity potential, $\Phi(\boldsymbol{x},t) \equiv \phi(\boldsymbol{x},\zeta,t)$, can be found from the free surface boundary conditions written (Zakharov 1968) in the form of

$$\frac{\partial \zeta}{\partial t} + \boldsymbol{\nabla}\Phi\cdot\boldsymbol{\nabla}\zeta = \left(1 + |\boldsymbol{\nabla}\zeta|^2\right) W\,, \tag{1}$$

$$\frac{\partial \Phi}{\partial t} + \tfrac{1}{2}|\boldsymbol{\nabla}\Phi|^2 + g\zeta = \tfrac{1}{2}\left(1 + |\boldsymbol{\nabla}\zeta|^2\right) W^2\,, \tag{2}$$

where $\boldsymbol{x} = (x,y)$ is the horizontal coordinates, g is the gravitational acceleration, and $W = \partial\phi/\partial z|_{z=\zeta}$ is the vertical velocity evaluated at the free surface located at $z=\zeta$. Notice that equations (1)–(2) can be considered as nonlinear evolution equations for ζ and Φ defined in the horizontal plane, once the expression for W is found in terms of ζ and Φ. An explicit expression for W was obtained first by West *et al.* (1987) for infinitely deep water using asymptotic expansion for small wave steepness. After expanding the free surface vertical velocity and the free surface velocity potential in Taylor series about the mean free surface, West *et al.* (1987) obtained a closed set of explicit nonlinear evolution equations. Dommermuth & Yue (1987) also adopted a similar idea with solving the resulting boundary value problems numerically at each order. This approach has been further extended to water of finite depth by Matsuno (1992), Craig & Sulem (1993), and Choi (1995), among others, with slightly different expansion methods.

Here, the original formulation of West *et al.* (1987) is further generalized to include slowly-varying surface currents and bottom topography effects by assuming the length scales of variation of surface currents and bottom topography are much greater than the peak wavelength, while their magnitudes of variation are allowed to be finite.

2 GOVERNING EQUATIONS

For an ideal fluid, we can introduce the velocity potential $\phi(\boldsymbol{x}, z, t)$ satisfying the Laplace equation:

$$\nabla^2\phi + \frac{\partial^2\phi}{\partial z^2} = 0 \qquad \text{for} \quad -h \le z \le \zeta(\boldsymbol{x}, t), \tag{3}$$

where $\zeta(\boldsymbol{x}, t)$ is the free surface elevation and the horizontal gradient $\boldsymbol{\nabla}$ is defined by

$$\boldsymbol{\nabla} = \left(\frac{\partial}{\partial x}, \frac{\partial}{\partial y}\right). \tag{4}$$

The bottom boundary condition is given by

$$\boldsymbol{\nabla}\phi\cdot\boldsymbol{\nabla}h + \frac{\partial\phi}{\partial z} = 0 \qquad \text{at} \quad z = -h. \tag{5}$$

At the free surface, the velocity potential ϕ and the surface elevation ζ satisfy the kinematic and dynamic free surface boundary conditions:

$$\zeta_t + \boldsymbol{u}\cdot\boldsymbol{\nabla}\zeta = w \qquad \text{at} \quad z = \zeta(\boldsymbol{x}, t), \tag{6}$$

$$\phi_t + \tfrac{1}{2}(\boldsymbol{\nabla}\phi)^2 + \tfrac{1}{2}{\phi_z}^2 + g\zeta = 0, \quad \text{at} \quad z = \zeta(\boldsymbol{x}, t), \tag{7}$$

where g is the gravitational acceleration and ρ is the fluid density.

By substituting $z = \zeta$ into (6) and (7), and using the following chain rules for differentiation,

$$\boldsymbol{\nabla}\phi|_{z=\zeta} = \boldsymbol{\nabla}\Phi - W\boldsymbol{\nabla}\zeta, \tag{8}$$

$$\left.\frac{\partial\phi}{\partial t}\right|_{z=\zeta} = \frac{\partial\Phi}{\partial t} - W\frac{\partial\zeta}{\partial t}, \tag{9}$$

where the free surface velocity potential Φ and the vertical velocity at the free surface W are defined by

$$\Phi(\boldsymbol{x}, t) \equiv \phi(\boldsymbol{x}, z = \zeta), \qquad W \equiv \left.\frac{\partial\phi}{\partial z}\right|_{z=\zeta}, \tag{10}$$

the free surface boundary conditions given by (6)–(7) can be re-written to the form given by (1)–(2) in terms of ζ, Φ, and W. If we can find the expression for W in terms of ζ and Φ, equations (1)–(2) will be a closed system for ζ and Φ.

3 EXPANSION METHOD FOR UNIFORM WATER DEPTH

3.1 PHYSICAL SPACE

First we consider the case of constant water depth, $\boldsymbol{\nabla}h = 0$. Expanding the free surface velocity potential Φ in (10) in Taylor series about the mean free surface yields

$$\Phi = \sum_{n=0}^{\infty} \mathcal{A}_n\big[\phi_0\big], \tag{11}$$

where operator $\mathcal{A}_n$ is defined by

$$\mathcal{A}_{2m} = (-1)^m \frac{\zeta^{2m}}{(2m)!}\triangle^m, \tag{12}$$

$$\mathcal{A}_{2m+1} = (-1)^{m+1} \frac{\zeta^{2m+1}}{(2m+1)!}\triangle^m\mathcal{L}. \tag{13}$$

In (12)–(13), we have used $\partial^2\phi/\partial z^2 = -\triangle\phi$ from (3), $\triangle = \nabla^2$, and

$$\phi_z(\boldsymbol{x}, 0, t) = -\mathcal{L}\big[\phi_0\big], \quad \phi_0 = \phi(\boldsymbol{x}, 0, t). \tag{14}$$

where $\mathcal{L}$ is the linear integral operator to be determined by solving the following linear boundary value problem:

$$\nabla^2\phi + \frac{\partial^2\phi}{\partial z^2} = 0 \qquad \text{for } -h \le z \le 0, \tag{15}$$

with the boundary conditions at $z = 0$ and $z = -h$ given by

$$\phi(\boldsymbol{x}, 0, t) = \phi_0(\boldsymbol{x}, t) \quad \phi_z(\boldsymbol{x}, -h, t) = 0. \tag{16}$$

Notice that the series given by (11) can be also inverted to

$$\phi_0 = \sum_{j=1}^{\infty} \Phi_j, \tag{17}$$

where

$$\Phi_j = -\sum_{l=1}^{j-1} \mathcal{A}_l\left[\Phi_{j-l}\right] \quad \text{for } j \ge 2, \quad \Phi_1 = \Phi. \tag{18}$$

Similarly, the vertical velocity at the free surface, W, can be expanded in Taylor series as

$$W = \sum_{n=1}^{\infty} W_n, \qquad W_n = \sum_{j=1}^{n} C_j\big[\Phi_{n-j}\big], \tag{19}$$

where Φ_n is given by (18) and operator $\mathcal{C}_n$ is defined by

$$\mathcal{C}_{2m} = (-1)^{m+1}\frac{\zeta^{2m}}{(2m)!}\triangle^m\mathcal{L}, \tag{20}$$

$$\mathcal{C}_{2m+1} = (-1)^{m+1}\frac{\zeta^{2m+1}}{(2m+1)!}\triangle^{m+1}. \tag{21}$$

Notice that $W_n = O(\epsilon^n)$ and $\Phi_n = O(\epsilon^n)$ with ϵ being the wave steepness defined by ϵ=wave amplitude/wave length, and they can be found recursively, as a function of ζ and Φ.

3.2 FOURIER SPACE

Suppose that all physical variables can be written in Fourier series

$$f(\boldsymbol{x}, t) = \sum_{n,m} a_{nm}(t)\, \mathrm{e}^{i(nk_1 x + mk_2 y)}, \tag{22}$$

and, then, the two linear operators in $\mathcal{A}_n$ and $\mathcal{C}_n$ can be written as

$$\triangle = -k^2, \qquad \mathcal{L} = -k \tanh(kh), \tag{23}$$

where

$$k^2 = (nk_1)^2 + (mk_2)^2.$$

By substituting (23) into (12)–(13) and (18), the expressions for Φ_n can be written explicitly as

$$\begin{aligned}
\Phi_1 &= \Phi, \\
\Phi_2 &= -\zeta k \tanh(kh)\, \Phi_1, \\
\Phi_3 &= -\zeta k \tanh(kh)\, \Phi_2 - \frac{1}{2!}\zeta^2 k^2 \Phi_1, \\
\Phi_n &= -\sum_{j=1}^{n-1} \mathcal{A}_j \left[\Phi_{n-j}\right] \quad \text{for } n \geq 2,
\end{aligned} \tag{24}$$

where $\mathcal{A}_n$ is given by

$$\begin{aligned}
\mathcal{A}_{2m} &= \frac{\zeta^{2m}}{(2m)!}\, k^{2m}, \\
\mathcal{A}_{2m+1} &= \frac{\zeta^{2m+1}}{(2m+1)!}\, k^{2m+1} \tanh(kh).
\end{aligned}$$

Similarly, the expansion for W in (19) can be found as

$$\begin{aligned}
W_1 &= k \tanh(kh)\, \Phi_1, \\
W_2 &= k \tanh(kh)\, \Phi_2 + \zeta k^2 \Phi_1, \\
W_3 &= k \tanh(kh)\, \Phi_3 + \zeta k^2 \Phi_2 + \frac{1}{2!}\zeta^2 k^3 \tanh(kh)\, \Phi_1, \\
W_n &= -\sum_{j=0}^{n-1} \mathcal{C}_j \left[\Phi_{n-j}\right] \quad \text{for } n \geq 1,
\end{aligned} \tag{25}$$

where operator $\mathcal{C}_n$ is given by

$$\begin{aligned}
\mathcal{C}_{2m} &= \frac{\zeta^{2m}}{(2m)!}\, k^{2m+1} \tanh(kh), \\
\mathcal{C}_{2m+1} &= \frac{\zeta^{2m+1}}{(2m+1)!}\, k^{2m+2}.
\end{aligned}$$

For infinitely deep water, $\tanh(kh) \to 1$ for two-dimensional waves and the system of West *et al* (1987) originally presented can be recovered while $\tanh(kh) \to \mathrm{sign}\,(k)$ for one-dimensional waves.

4 NONLINEAR EVOLUTION EQUATIONS

Now Φ_n and W_n are written explicitly in ζ and Φ and, by substituting (19) or (25) for W into (1)–(2), we have a closed system of nonlinear evolution equations for ζ and Φ, in either physical or Fourier space, in the form of:

$$\frac{\partial \zeta}{\partial t} = \sum_{n=1}^{\infty} \mathrm{Q}_n(\zeta, \Phi)\,, \qquad \frac{\partial \Phi}{\partial t} = \sum_{n=1}^{\infty} \mathrm{R}_n(\zeta, \Phi)\,. \tag{26}$$

where Q_n and R_n representing the terms of $O(\epsilon^n)$ are given by

$$\begin{aligned}
&\mathrm{Q}_1 = W_1, \quad \mathrm{Q}_2 = W_2 - \boldsymbol{\nabla}\Phi \cdot \boldsymbol{\nabla}\zeta, \\
&\mathrm{Q}_n = W_n + |\boldsymbol{\nabla}\zeta|^2 W_{n-2} \quad \text{for } n \geq 3,
\end{aligned} \tag{27}$$

$$\begin{aligned}
\mathrm{R}_1 &= -g\zeta, \quad \mathrm{R}_2 = -\tfrac{1}{2}|\boldsymbol{\nabla}\Phi|^2 + \tfrac{1}{2}{W_1}^2, \quad \mathrm{R}_3 = W_1\, W_2, \\
\mathrm{R}_n &= \tfrac{1}{2}\sum_{j=0}^{n-2} W_{n-j-1}\, W_{j+1} \\
&\qquad + \tfrac{1}{2}|\boldsymbol{\nabla}\zeta|^2 \sum_{j=0}^{n-4} W_{n-j-3}\, W_{j+1} \quad \text{for } n \geq 4.
\end{aligned} \tag{28}$$

Notice that the leading-order terms (Q_1 and R_1) represent linear dispersive effects while Q_n and R_n for $n \geq 2$ describe higher-order dispersive effects and nonlinear wave-wave interaction. Alternatively, the resulting system can be obtained by expanding the Dirichlet-Neumann operator, as suggested by Craig & Sulem (1993).

5 NUMERICAL METHODS AND VALIDATION WITH FULLY NONLINEAR SOLUTIONS FOR ONE-DIMENSIONAL WAVES

For numerical computations, the right-hand sides of the system given by (26) are truncated to some finite order of wave steepness and, then, are evaluated via a pseudo-spectral method based on the Fast Fourier Transform. So the surface elevation ζ and the free surface velocity potential Φ are represented by double Fourier series:

$$(\zeta, \Phi) = \sum_{n=-\frac{N_1}{2}}^{\frac{N_1}{2}} \sum_{m=-\frac{N_2}{2}}^{\frac{N_2}{2}} \Big(a_{nm}, b_{nm}\Big)\, \mathrm{e}^{ink_1 x + imk_2 y}, \tag{29}$$

where $a_{nm}(t)$ and $b_{nm}(t)$ are the Fourier coefficients to be found, N_1 and N_2 are the numbers of Fourier modes in the x- and y-directions, respectively, and $k_1 = 2\pi/L_1$

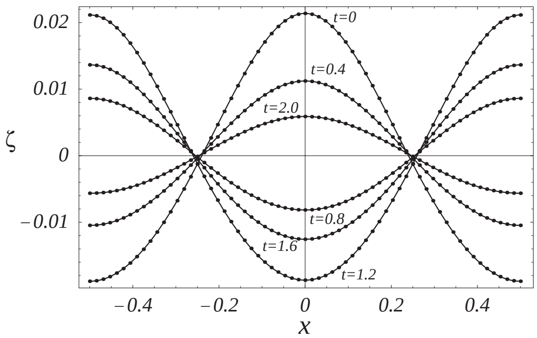

(a)

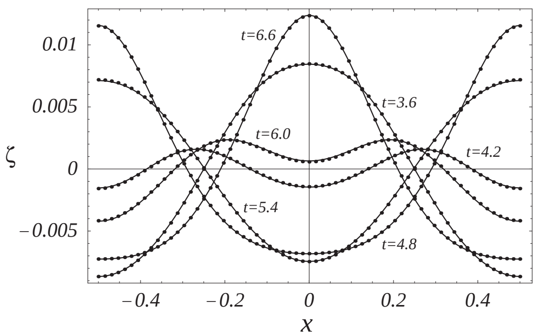

(b)

Figure 1: Comparison between numerical solutions of the truncated fifth-order system (dots) given by (26) and the fully nonlinear Euler equations (solid lines) for a periodic standing wave. (a) $h/\lambda = 1$ with the third-order Stokes wave solution of wave amplitude $a/\lambda = 0.02$ for ζ and $\Phi = 0$ as initial conditions. (b) $h/\lambda = 0.1$ with the linear wave solution of wave amplitude $a/\lambda = 0.01$ for ζ and $\Phi = 0$.

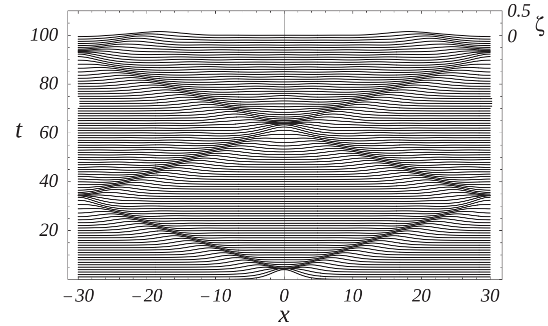

(a)

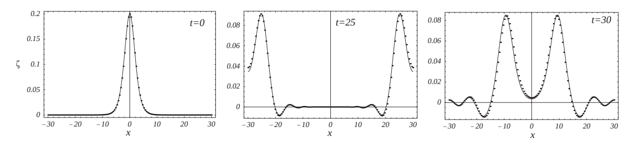

(b)

Figure 2: (a) Time evolution of a KdV solitary wave of wave amplitude $a/h = 0.2$ in a periodic domain. In this computation, the number of Fourier modes of $N_x = 2^8$ and the initial conditions are $\zeta(x, 0) = \zeta_{KdV}(x)$ and $\Phi = 0$. (b) Comparison between numerical solutions of the truncated fifth-order system (dots) given by (26) and the fully nonlinear Euler equations (solid lines) at three different times.

and $k_2 = 2\pi/L_2$ with L_1 and L_2 being the computational domain lengths in the x- and y-directions, respectively. Then, the evolution equations are integrated in time using the fourth-order Runge-Kutta method. More explanations about the numerical method can be found in Choi, Kent & Schillinger (2005).

In this section, we consider one-dimensional waves to validate our numerical solutions of the truncated system given by (26) with those of the exact evolution equations derived from the Euler equations without any approximation (Dyachenko *et al.* 1996; Choi & Camassa 1999). This fully nonlinear theory is based on the conformal mapping technique and can be applicable only to two-dimensional flow (or one-dimensional waves). The details of the numerical method for the exact evolution equations can be found in Li, Hyman & Choi (2004). In our computations, we choose $g = 1$ and $\lambda = 1$ (or $h = 1$). The number of Fourier modes is $N_x = 2^8$ and the time step is $\Delta t = 0.01$.

Figure 1 shows an example of comparisons between numerical solutions of the fifth-order nonlinear evolution equations and the fully nonlinear Euler equations for one-dimensional periodic standing waves for two different depths of $h/\lambda = 1$ and $h/\lambda = 0.1$. Notice that, even with for the lower-order (e.g. third-order) nonlinear evolution equations, the two solutions are indistinguishable to graphical accuracy. From figure $1(b)$, it can be seen that, as the water depth decreases, nonlinear effects become more important and the higher-harmonic components are easily amplified.

For another validation of our numerical method for the finite-depth formulation, we consider the propagation and collision of solitary waves in shallow water, as shown in figure 2. Initially, a Korteweg-de Vries (KdV) solitary wave given by $\zeta_{KdV}(x) = a\,\mathrm{sech}^2(x/l)$ with $l^2 = 4h/(3a)$ is located at the center of the computational domain. Since $\Phi = 0$ at $t = 0$, a single solitary wave is disintegrated into two solitary waves propagating in opposite directions and colliding with solitary waves propagating from neighboring computational domains due to our periodic boundary conditions. Once again, the two solutions show good agreement, as shown in figure 2.

6 EFFECTS OF SLOWLY-VARYING CURRENTS

Consider a two-dimensional horizontal surface current, $\boldsymbol{U} = \boldsymbol{U}(\boldsymbol{x})$, which is assumed to vary slowly so that $\lambda(\boldsymbol{\nabla}\cdot\boldsymbol{U})/|\boldsymbol{U}| = O(\mu)$, where $\mu = \lambda/L$ is a small parameter representing the slow variation of the current, with λ being the typical wavelength and L being the characteristic length of current variation. By assuming that $U_y - V_x = O(\mu^2)$ at $t = 0$, it can be shown that the vorticity is $O(\mu^2)$ for all t. This implies that all perturbations to this current field will be irrotational with an error of $O(\mu^2)$. Therefore, by adopting an expansion method similar to that introduced in sec. 3, it can be shown that the nonlinear evolution equations given by (26) are slightly modified, with an error of $O(\epsilon^2)$, to

$$\frac{\partial\zeta}{\partial t} + \boldsymbol{\nabla}\cdot(\boldsymbol{U}\,\zeta) = \sum_{n=1}^{\infty} \mathrm{Q}_n[\zeta, \Phi]\,, \tag{30}$$

$$\frac{\partial\Phi}{\partial t} + \boldsymbol{U}\cdot\boldsymbol{\nabla}\Phi = \sum_{n=1}^{\infty} \mathrm{R}_n[\zeta, \Phi]\,. \tag{31}$$

A more classical approach to study wave-current interaction is to use the wave action model. For a slowly-varying *linear* wave train, it is well-known that the surface elevation ζ can be approximated by

$$\zeta = a(\boldsymbol{x}, t)\,\mathrm{e}^{\mathrm{i}\theta(\boldsymbol{x},t)}, \tag{32}$$

where the slowly-varying local amplitude $a(\boldsymbol{x}, t)$ and local wave number $\boldsymbol{k}(\boldsymbol{x}, t) \equiv \boldsymbol{\nabla}\theta$ then can be found by solving the wave action equation and the kinematic equation, respectively, (Bretherton & Garrett 1969; Phillips 1977):

$$\frac{\partial(a^2/\sigma)}{\partial t} + \boldsymbol{\nabla}\cdot\left[(\boldsymbol{c}_g + \boldsymbol{U})\,(a^2/\sigma)\right] = 0, \quad \frac{\partial\boldsymbol{k}}{\partial t} + \boldsymbol{\nabla}\omega = 0. \tag{33}$$

In equation (33), the group velocity c_g and the local wave frequency $\omega(\boldsymbol{k}, \boldsymbol{x}, t) \equiv -\theta_t$ can be found from

$$c_g = \frac{\partial\sigma}{\partial k}, \quad \omega = \sigma + \boldsymbol{k}\cdot\boldsymbol{U}, \quad \sigma^2 = gk. \tag{34}$$

As a special case, when the local wave amplitude and wave number remain unchanged in time, the wave action model (33) can be further simplified to

$$(c_g + U)\,(a^2/\sigma) = \text{constant}, \quad \sigma + k_x U = \text{constant}. \tag{35}$$

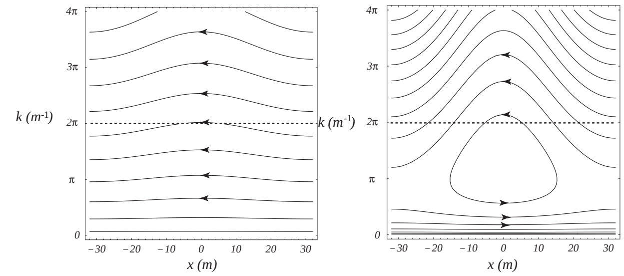

(a) (b)

Figure 3: Variation of the local wave number $k(x)$ predicted by the steady kinematic equation given by (35) for (a) waves traveling to the left (case 1) and (b) waves traveling to the right (case 2) in the absence of surface current. The dashed lines represent the initial wave number of the uniform wave train whose wave amplitude and wavelength are 1cm and 1m, respectively.

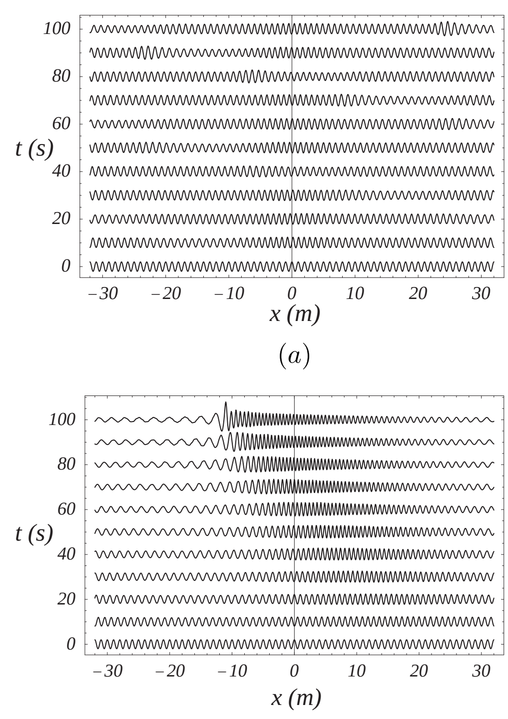

Figure 4: Numerical solutions of the nonlinear evolution equations given by (30)–(31) for surface elevation $\zeta(x, t)$: (a) a uniform wave train traveling to the left (case 1); (b) a uniform wave train traveling to the right (case 2). Initially, the wave amplitude and wavelength of the uniform wave train are 1cm and 1m, respectively.

In this paper, to demonstrate consistency of the nonlinear evolution equations given by (30)–(31) with the wave action model in (33), we consider a simple one-dimensional surface current:

$$U(x) = U_0 + U_1 \cos^2(\pi x/L) \qquad \text{for } -L/2 \leq x \leq L/2, \tag{36}$$

with the following dimensional parameters: U_0= -1 m/s, U_1= 0.2 m/s, and L = 64 m and study the evolution of initially monochromatic wave trains with a wavelength of 1 m and an amplitude of 1 cm propagating in the both negative (case 1) and positive (case 2) x-directions in the absence of surface current. The number of Fourier modes in our computations is 2^{10} (with the number of grid points per wavelength being 16) and the time step is Δt=0.01 sec.

Before making detailed comparisons between numerical solutions of the nonlinear evolution equations and the wave action equation, the changes in the local wave number are calculated from equation (35) (obtained under the steady assumption which might not be valid here) and are presented in figure 3. These steady solutions indicate that for the wave train propagating in the negative x-direction the wavenumber and the wave amplitude both increase slightly when interacting with the current. For the wave train propagating in the +x-direction, figure 3 shows that the wavenumber and amplitude increase considerably and, as indicated by the closed trajectories in figure 3(b), some wave groups are trapped inside the computational domain.

As shown in figure 4, the numerical solutions of the nonlinear evolution equations given by (30)–(31) show that an initially uniform wave train traveling in the negative x direction experiences a slight modulation in wave amplitude and wave number, in agreement with figure 3(a) expects. On the other hand, for waves traveling in the $+x$ direction, the wave steepness increases steadily in time, as shown in Figure 4(b) until t=100s at which time the simulation was terminated. At about this same time, a singularity also develops in the solution of (33) due to the convergence of two wave trains with different wavenumbers at the same location. Thus, the narrow-band assumption expressed by equation (32) appears to break down at this point.

As shown in figures 5 and 6, numerical solutions of (30)–(31) for the local wave number and local wave amplitude compare well with those of (33). Surface waves propagating in the negative x-direction experience fairly small and quasi-time-periodic perturbations (because of the periodic boundary conditions), while the local wave amplitude and local wave number for surface waves propagating in the positive x direction increases.

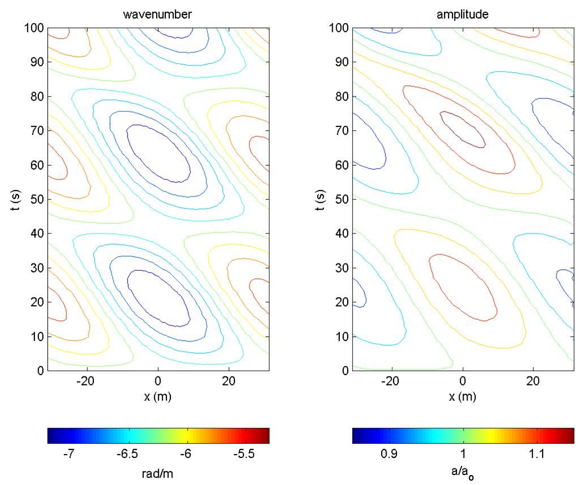

(a)

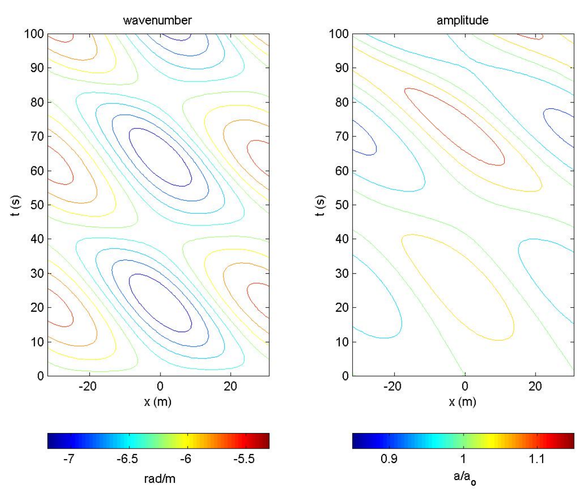

(b)

Figure 5: Evolution of the local wave number $k(x, t)$ and the local wave amplitude ratio defined by $a(x, t)/a_0$ for the waves traveling in the negative x-direction (case 1): (a) the nonlinear surface wave model given by (30)–(31); (b) the kinematic and wave action equations given by (33). These results correspond to the numerical solution shown in figure 4(a).

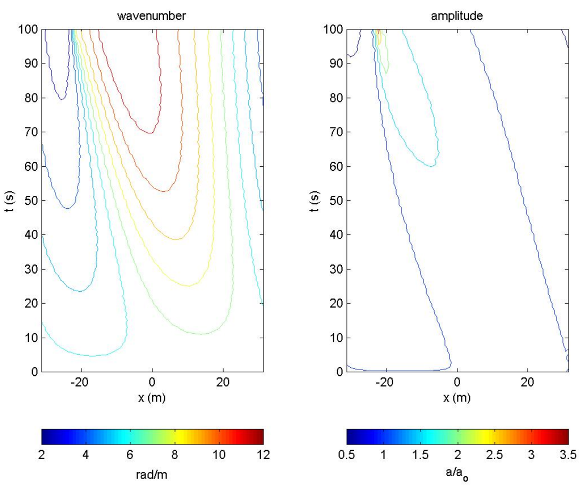

(a)

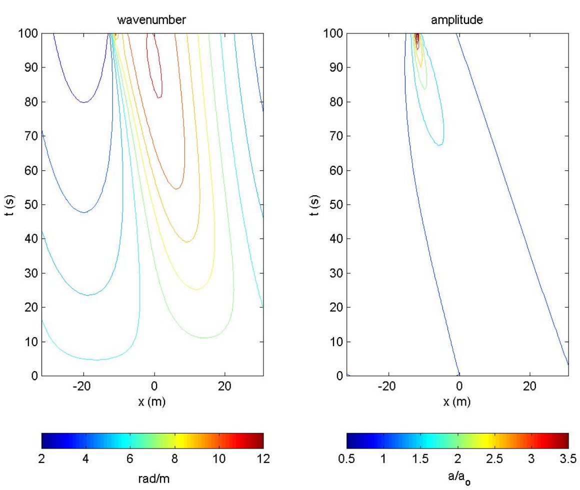

(b)

Figure 6: Evolution of the local wave number $k(x,t)$ and the local wave amplitude ratio defined by $a(x,t)/a_0$ for the waves traveling in the positive x-direction (case 2): (a) the nonlinear surface wave model given by (30)–(31); (b) the kinematic equation given by (33). These results correspond to the numerical solution shown in figure 4(b).

7 EFFECTS OF SLOWLY-VARYING BOTTOM TOPOGRAPHY

The system given by (26) can be further generalized to include the effects of slowly-varying bottom topography of arbitrary amplitude. By assuming that the local water depth $h(\boldsymbol{x})$ varies slowly so that $\mu = \lambda|\boldsymbol{\nabla} h|/h \ll 1$ and substituting into (3)–(7) the following transformations:

$$\bar{x} = \int_{x_0}^{x} \eta(x', y)\,\mathrm{d}x', \;\; \bar{y} = \int_{y_0}^{y} \eta(x, y')\,\mathrm{d}y', \;\; \bar{z} = \eta(\boldsymbol{x})z,$$

where $\eta = h_0/h(\boldsymbol{x})$ and h_0 is the local water depth at $x = x_0$, the boundary value problem for $\phi(\overline{\boldsymbol{x}}, \bar{z})$ in the transformed horizontal domain becomes, with an error of $O(\mu)$,

$$\left(\overline{\nabla}^2 + \frac{\partial^2}{\partial \bar{z}^2}\right)\phi = 0 \quad \text{in } -h_0 < \bar{z} < 0, \tag{37}$$

$$\frac{\partial \phi}{\partial \bar{z}} = 0 \quad \text{at } \bar{z} = -h_0, \tag{38}$$

$$\frac{\partial \zeta}{\partial t} + \eta^2\, \overline{\boldsymbol{\nabla}}\phi\boldsymbol{\cdot}\overline{\boldsymbol{\nabla}}\zeta = \eta\left(\frac{\partial \phi}{\partial \bar{z}}\right) \quad \text{at } \bar{z} = \eta(\overline{\boldsymbol{x}})\,\zeta(\overline{\boldsymbol{x}}, t), \tag{39}$$

$$\frac{\partial \phi}{\partial t} + \tfrac{1}{2}\eta^2|\overline{\boldsymbol{\nabla}}\phi|^2 + \tfrac{1}{2}\eta^2\left(\frac{\partial \phi}{\partial \bar{z}}\right)^2 + g\zeta = 0 \quad \text{at } \bar{z} = \eta(\overline{\boldsymbol{x}})\,\zeta(\overline{\boldsymbol{x}}, t), \tag{40}$$

where $\overline{\boldsymbol{\nabla}} = (\partial/\partial\bar{x}, \partial/\partial\bar{y})$. Then, using the chain rules for differentiation in (8)–(9), the free surface boundary conditions given by (39)–(40), under the same order of approximation, can be also re-written as

$$\frac{\partial \zeta}{\partial t} + \eta^2\overline{\boldsymbol{\nabla}}\Phi\boldsymbol{\cdot}\overline{\boldsymbol{\nabla}}\zeta = \eta\left(1 + \eta^2|\overline{\boldsymbol{\nabla}}\zeta|^2\right)W\,, \tag{41}$$

$$\frac{\partial \Phi}{\partial t} + \tfrac{1}{2}\eta^2|\overline{\boldsymbol{\nabla}}\Phi|^2 + g\zeta = \tfrac{1}{2}\eta^2\left(1 + \eta^2|\overline{\boldsymbol{\nabla}}\zeta|^2\right)W^2\,. \tag{42}$$

Compared with those for constant water depth ($\eta = 1$ and $\overline{\boldsymbol{x}} = \boldsymbol{x}$) given by (1)–(2), the free surface boundary conditions are slightly modified, but the governing equation and the bottom boundary conditions are identical to those for constant water depth in (3) and (5). Therefore, it can be shown that a system of nonlinear evolution equations for $\zeta(\overline{\boldsymbol{x}}, t)$ and $\Phi(\overline{\boldsymbol{x}}, t)$ in the transformed domain can be obtained using the similar expansion technique as for constant water depth.

The expansions for Φ and W and the expressions for $\mathcal{A}_n$ and $\mathcal{C}_n$ in § 3 remain unchanged when replacing ζ, h, and $\boldsymbol{\nabla}$ by

$$\zeta \rightarrow \eta\,\zeta, \qquad h \rightarrow h_0, \qquad \boldsymbol{\nabla} \rightarrow \overline{\boldsymbol{\nabla}}. \tag{43}$$

The resulting nonlinear evolution equations for ζ and Φ in the transformed plane become

$$\frac{\partial \zeta}{\partial t} = \sum_{n=1}^{\infty} \overline{\mathrm{Q}}_n(\zeta, \Phi)\,, \qquad \frac{\partial \Phi}{\partial t} = \sum_{n=1}^{\infty} \overline{\mathrm{R}}_n(\zeta, \Phi)\,, \tag{44}$$

where $\overline{\mathrm{Q}}_n$ and $\overline{\mathrm{R}}_n$ representing the terms of $O(\epsilon^n)$ are given by

$$\overline{\mathrm{Q}}_1 = \eta W_1, \quad \overline{\mathrm{Q}}_2 = \eta W_2 - \eta^2 \overline{\boldsymbol{\nabla}}\Phi \cdot \overline{\boldsymbol{\nabla}}\zeta,$$
$$\overline{\mathrm{Q}}_n = \eta W_n + \eta^3 |\overline{\boldsymbol{\nabla}}\zeta|^2 W_{n-2} \quad \text{for } n \geq 3,$$

$$\overline{\mathrm{R}}_1 = -g\zeta, \quad \overline{\mathrm{R}}_2 = -\tfrac{1}{2}\eta^2 |\overline{\boldsymbol{\nabla}}\Phi|^2 + \tfrac{1}{2}\eta^2 {W_1}^2,$$
$$\overline{\mathrm{R}}_3 = \eta^2 W_1\, W_2,$$
$$\overline{\mathrm{R}}_n = \tfrac{1}{2}\sum_{j=0}^{n-2} \eta^2 W_{n-j-1}\, W_{j+1}$$
$$+\tfrac{1}{2}\eta^4 |\overline{\boldsymbol{\nabla}}\zeta|^2 \sum_{j=0}^{n-4} W_{n-j-3}\, W_{j+1} \quad \text{for } n \geq 4.$$

Notice that it is convenient to solve the system numerically in the transformed domain and to transform the numerical solutions back to the physical domain at the end of computations. To test our formulation and numerical method, we consider two examples in this paper using bottom topography given by

$$b(x) = \begin{cases} b_0 \cos^2\left(\frac{\pi x}{2 x_0}\right) & \text{for } |x| \leq x_0 \\ 0 & \text{for } |x| \geq x_0 \end{cases}. \tag{45}$$

In figure 7, it is shown that the system given by (41)–(42) can describe the well-known long wave phenomenon of generation of upstream-propagating solitary waves in shallow water, first observed numerically by Wu & Wu (1982) using the Boussinesq equations, with a uniform stream velocity U close to the linear long wave speed ($c_0 = \sqrt{g h_0}$). It is also shown that the system can be used to study refraction of short surface waves in water of finite depth, as can be seen in figure 7(b).

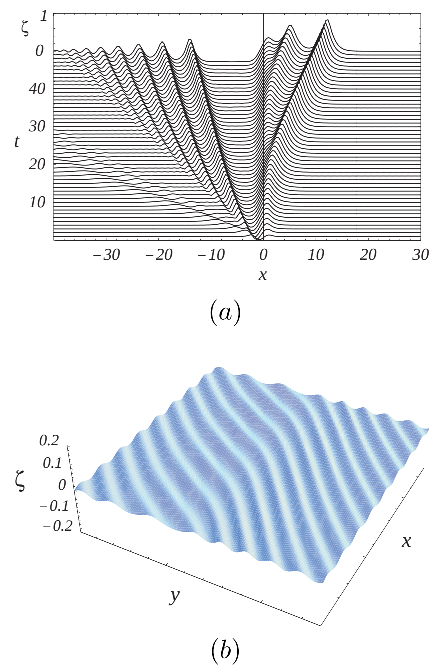

Figure 7: (a) Generation of one-dimensional forced solitary waves by bottom topography given by (45) with b_0/h_0=0.2 and $x_0/h_0 = 2$ in a uniform stream of $U/\sqrt{g h_0} = 1$. (b) Propagation of two-dimensional uniform wave train of wave amplitude $a/\lambda = 0.02$ over bottom topography of $h_0/\lambda = 0.4$, $b_0/\lambda = 0.3$, and $x_0/\lambda = 8$ at $t/\sqrt{\lambda/g} = 10$.

8 CONCLUSION

We derive a system of nonlinear evolution equations written in infinite series to describe the evolution of nonlinear surface waves interacting with surface currents in water of variable depth. For constant water depth, the truncated system is solved numerically using a pseudo-spectral method for periodic standing waves and solitary waves, and its numerical solutions are validated with numerical solutions of the fully nonlinear Euler equations. For wave-current interaction, our numerical solutions are consistent with numerical solutions of the wave action model. It has been shown that the formulation can be really generalized to the case of nonuniform water depth using a simple transformation and the evolution equations written in the transformed domain has the variable coefficients.

ACKNOWLEDGEMENTS

This work was supported by the US Office of Naval Research through Grants N00014-05-1-0537 and N00014-05-1-0273. The authors thank Caleb Schillinger for his help in computing the results shown in §6.

REFERENCES

Bretherton, F.P. and Garrett, C.J.R., "Wavetrains in inhomogeneous moving media," Proc. Roy. Soc. A, Vol. 302, 1969, pp. 529–554.

Choi, W., "Nonlinear evolution equations for two-dimensional surface waves in a fluid of finite depth," J. of Fluid Mech., Vol. 295, 1995, pp. 381–394.

Choi, W. and Camassa, R., "Exact evolution equations for surface waves," J. Eng. Mech., Vol. 125, 1999, pp. 756–760.

Choi, W., Kent, C.P. and Schillinger, C.J., "Numerical modeling of nonlinear surface waves and its validation," Advances in Engineering Mechanics - Reflections and outlooks in honor of Theodore Y.-T. Wu (ed. by A.T. Chwang, M.H. Teng & D.T. Valentine), World Scientific Publishing, 2005, pp. 94–110.

Craig, W. and Sulem, C., "Numerical simulation of gravity waves," J. Comput. Phys., Vol. 108, 1993, pp. 73–83.

Dommermuth, D. G. and Yue, D. K. P., "A higher-order spectral method for the study of nonlinear gravity waves," J. of Fluid Mech., Vol. 184, 1987, pp. 267–288.

Dyachenko, A. L., Zakharov,V. E., and Kuznetsov, E. A., "Nonlinear dynamics of the free surface of an ideal fluid," Plasma Phys. Rep., Vol. 22, 1996, pp. 916–928.

Li, Y. A., Hyman, J. M. and Choi, W., "A numerical study of the exact evolution equations for surface waves in water of finite depth," Studies in Applied. Math., Vol. 113, 2004, pp. 303–324.

Matsuno, Y., "Nonlinear evolutions of surface gravity waves on fluid of finite depth," Phys. Rev. Lett., Vol. 69, 1992, 609–611.

Phillips, O.M. The Dynamics of the Upper Ocean., 2nd ed., Cambridge University Press, Cambridge. 1977.

West, B. J., Brueckner, K. A., Janda, R. S., Milder, D. M. and Milton, R. L. A New Numerical method for Surface Hydrodynamics. J. Geophys. Res., Vol. 92, 1987, 11,803–11,824.

Wu, D.-M. and Wu, T. Y. "Three-dimensional nonlinear long waves due to moving surface pressure," Proc. the 14th Symp. on Naval hydrodynamics,1982,103–129.